Discriminating Between Input Signals Via Single Neuron Activity

Jianfeng Feng*,** Feng Liu*,***

*COGS, University of Sussex at Brighton, BN1 9QH, UK

**Newton Institute, Cambridge University, CB3 0EH, UK

*** Department of Physics, Nanjing University, Nanjing 210093, P.R.China

jianfeng@cogs.susx.ac.uk http://www.cogs.susx.ac.uk/users/jianfeng

Abstract

What is neuronal capability of discriminating between different input signals? Furthermore, how to improve its discriminating capability? We explore these issues both theoretically and numerically for the integrate-and-fire (IF) model and the IF-FHN model (a simplified version of the FitzHugh-Nagumo model [6]). It is found that adding correlations and increasing inhibitory inputs considerably reduce the total probability of misclassifications (TPM). A novel theory on discrimination tasks is developed and the theory accounts for all observed numerical results.

1 Introduction

To efficiently discriminate between different input signals, for example to tell the image of a prey from that of a predator, is of vital importance to a nervous system. The actual neuron mechanisms underpinning the cognitive activity remain one of the most significant and puzzling problems in neuroscience, despite there have been mounting experimental and theoretical results devoted to the topic (for example see recent reviews [14, 15]). In a series of experiments, Newsome and his colleagues have compared single neuron activity with psychophysical experiment data. They found, surprisingly,

that the information extracted from single neuron activity in MT is almost enough to account for psychophysical experiment data. Hence an observation of the firing rates of single neuron, at least in MT, contains enough information to further guide motor activity. Imagining the enormous number of neurons in the cortex, their findings are striking and open up many interesting issues for further theoretical and experimental study. Interestingly, similar findings are reported in somatosensory pathways [15] as well. In line with these experimental results, in this paper we concentrate on the relationship of the input and output firing rates of a single neuron. The issue we are going to address is quite straightforward (see Fig. 1). Suppose that a neuron receives two set

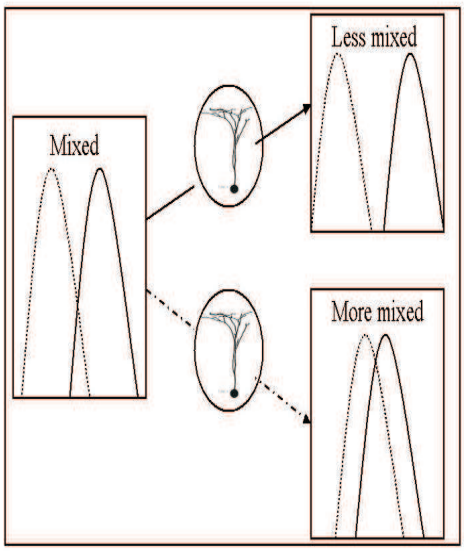

Figure 1: For two mixed signals (left), after neuronal transformation, will they become more mixed or more separated?

of signals (coded by firing rates) distributed according to two histograms as depicted in Fig. 1 (left). Will the signals become more mixed or separated, after neuronal transformations?

More specifically we consider neuron models with a combination of (coherent) signal inputs and masking 'noise' inputs. The models we employ here are the integrate-and-

fire(IF) model and the IF-FHN model [6]. We find that with a small fraction of signal inputs, the efferent spike trains of the model contain enough information to discriminate between different inputs (see below for more details).

We then explore the possible functional role of inhibitory inputs on discrimination tasks. A neuron extensively receives both excitatory and inhibitory inputs. It is clear that the excitatory input codes the input information: the stronger the stimuli are, the faster the neuron fires. Less is known about the inhibitory input, much as different, theoretical hypotheses have been put forward in the literature ranging from actually synchronizing the firing of a group of neurons [20], linearizing input-output relationship [7] and increasing neuron firing rates [6] etc. We find that adding certain amount of inhibitory inputs considerably enhances the neuronal discrimination capability if signal inputs are correlated.

The conclusion above seems quite counter intuitive. We all know that increasing inhibitory inputs to a single neuron model will result in an increase on the variability of its efferent spike trains [6]. The histogram of firing rates will thus become more spread out and, as a consequence, the discrimination of different inputs becomes more difficult. However, this is not the case. To understand the mechanism underpinning the observed phenomena, we then go a step further to theoretically explore the model behaviour. Based upon the IF model, a theory on discrimination tasks is developed. We find that two key mechanisms for achieving a better separation of output signals, in comparison with input signals, are

1. input signals are positively correlated and

2. excitatory inputs and inhibitory inputs are exactly balanced.

Without correlations, no matter how strong the inhibitory inputs are, the separability of the output signals and the input signals is identical: if the input signals are separable, so are the output signals and vise versa. With correlations, the stronger the inhibitory inputs are, the better the separation.

Theoretically the critical value of the coherent inputs at which the output histograms are separable is exactly obtained (Theorem 2) for the case of correlated and exactly balanced inputs (the most interesting case). The results enable us to assess the dependence of our conclusions on different model parameters and input signals. It is illuminating to see that the critical value is independent of model parameters including the threshold, the decay time and the EPSP and IPSP magnitude.

All the aforementioned results are obtained for the IF and IF-FHN model without reversal potentials, we further examine our conclusions for the IF model with reversal potentials. Since adding reversal potentials to a model is equivalent to increasing its decay rate (depending on input signals), we would naturally expect that the model with reversal potentials will become more effectively to distinguish different inputs. The conclusion is numerically confirmed.

During the past few years, inhibitory inputs (see for example [11, 12]) and correlated inputs (see for example [17, 18] are two topics widely investigated in neuroscience. It seems it is generally accepted that they play important roles in information processing in the brain. Our results here provide a convincing and direct evidence to show that they do improve the performance of a single neuron. Such results would also be valuable on practical applications of spiking neural networks [9].

2 The Integrate-and-fire Model and its Inputs

The first neuron model we use here is the classical IF model [4, 5, 19]. When the membrane potential V_t is below the threshold V_{thre}, it is given by

$$dV_t = -L(V_t - V_{rest})dt + dI_{syn}(t) \tag{2.1}$$

where L is the decay coefficient and the synaptic input is

$$I_{syn}(t) = a\sum_{i=1}^{p} E_i(t) - b\sum_{j=1}^{q} I_j(t)$$

with $E_i(t), I_i(t)$ as Poisson processes with rate $\lambda_{i,E}$ and $\lambda_{i,I}$ respectively, $a > 0, b > 0$ are magnitude of each EPSP and IPSP, p and q are the total number of active excitatory and inhibitory synapses. Once V_t crosses V_{thre} from below a spike is generated and V_t is reset to V_{rest}, the resting potential. This model is termed the IF model. The interspike interval of efferent spikes is

$$T = \inf\{t : V_t \geq V_{thre}\}$$

More specifically, synaptic inputs take the following form ($p = q$)

$$\begin{aligned} I_{syn}(t) &= a\sum_{i=1}^{p} E_i(t) - b\sum_{j=1}^{p} I_j(t) \\ &= a\sum_{i=1}^{p_c} E_i(t) + a\sum_{i=p_c+1}^{p} E_i(t) - b\sum_{i=1}^{p_c} I_i(t) - b\sum_{i=p_c+1}^{p} I_i(t) \end{aligned}$$

where $E_i(t), i = 1, \cdots, p_c$ are correlated Poisson processes with an identical rate $\lambda_j, j = 1, 2$, $E_i(t)$ is Poisson processes with a firing rate ξ_{i-p_c} independently and identically distributed random variables from $[0, 100], i = p_c + 1, \cdots, p$, $I_i(t), i = 1, \cdots, p$ have the same property as $E_i(t)$, but with a firing rate of $r\lambda_j, j = 1, 2$ or $r\xi_{i-p_c}$ for $r \in [0, 1]$ representing the ratio between inhibitory and excitatory inputs.

From now on, we further use diffusion approximations to approximate synaptic inputs [19] and without loss of generality we assume that $a = b$ and $V_{rest} = 0$.

$$\begin{aligned} I_{syn}(t) &= ap_c\lambda_j t + a\sum_{i=1}^{p-p_c} \xi_i t - bp_c r\lambda_j t - b\sum_{i=1}^{p-p_c} r\xi_i t \\ &\quad + \sqrt{(a^2 + b^2 r)\lambda_j p_c(1 + c(p_c - 1)) + (a^2 + b^2 r)\sum_{i=1}^{p-p_c} \xi_i} \cdot B_t \end{aligned}$$

where B_t is the standard Brownian motion and $j = 1, 2$. We first consider the case that a neuron receives independent inputs. As we might expect, the output from a single neuron does not contain enough information for the discrimination task (results not shown, see next section), with the ratio of inhibitory to excitatory inputs spanned from nil to one (exactly balanced inhibitory and excitatory input). We then turn to the situation that a small amount of correlations are added to the synaptic inputs which code coherently moving dots. For the simplicity of notation we assume that the

correlation coefficient between ith excitatory (inhibitory) synapse and jth excitatory (inhibitory) synapse is $c > 0$. The correlation considered here reflects the correlation of activity of different synapses, as discussed and explored in [6, 21]. It is not the correlation of single incoming EPSP or IPSP which could be expressed as $c_{ij}(t - t')$ for the EPSP (IPSP) at time t of the ith synapse and time t' of the jth synapse. We refer the reader to [6] for a detailed discussion on the meaning of the correlation considered here.

In summary, suppose that a neuron receives p synaptic inputs. The goal of the postsynaptic neuron is to discriminate between two types of inputs

1. p_c excitatory Poisson inputs fire at a rate λ_1 and

   p_c inhibitory Poisson inputs fire at a rate $r\lambda_1$ with $r \in [0, 1]$;

2. p_c excitatory Poisson inputs fire at a rate λ_2 ($\lambda_2 \neq \lambda_1$)

   p_c inhibitory Poisson inputs fire at a rate $r\lambda_2$ with $r \in [0, 1]$.

In both cases, the neuron receives 'noise' Poisson inputs consisted of $p - p_c$ excitatory inputs and the same number of inhibitory inputs. We assume that 'noise' excitatory inputs are uniformly distributed between 0 and 100 Hz, and 'noise' inhibitory inputs are between 0 and $100r$ Hz. Without loss of generality, we always assume that $\lambda_2 > \lambda_1$.

3 Numerical Results

Example 1 The setup above actually (see Fig. 2) mimics the inputs to an MT neuron used in the experiments. In the experiment of Newsome and his colleagues, the input image is a collection of moving dots, say p dots. p_c out of p dots move with an identical (coherent) direction, either upward or downward and $p - p_c$ dots move with random directions. In the literature [2], p_c/p is called coherence level. We could assume that an MT neuron exclusively receives information of motion directions of an input image (moving dots), i.e. the cell receives p synaptic inputs, each represents the moving

direction of a dot. Denote that $N_i(t), i = 1, \cdots, p$ as a Poisson process with a rate ζ_i, where ζ_i takes value from $[0, 100]$Hz, i.e. $(\zeta_i/100)2\pi$ is the motion direction of the i-th random moving dot (see [2]) and the motion of each dot is coded by the firing rate of a single synaptic (Poisson) input. Hence $\zeta_i = \lambda_1 = 25$ Hz represents the input of upward motion, or the ith dot moves upward; $\zeta_i = \lambda_2 = 75$ Hz represents the downward motion. For example when the neuron receives synaptic inputs with a coherence of p_c/p, which

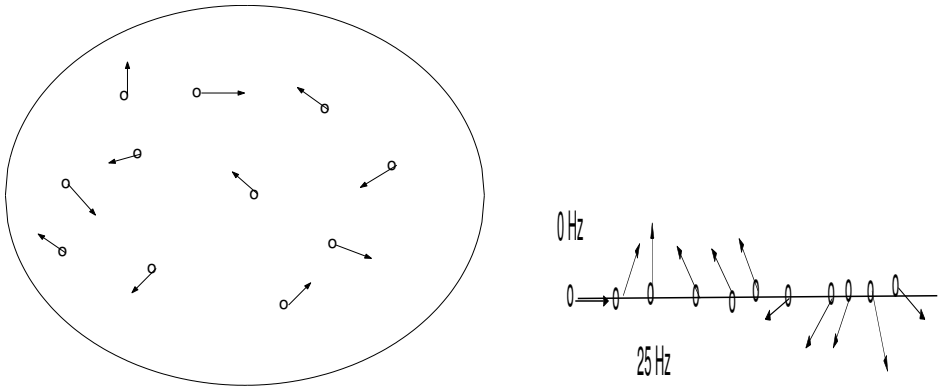

Figure 2: Schematic plot of inputs used in the experiment (see [2], left) and in the model (right). In the model, the dot moves horizontally towards right is represented by synaptic inputs of 0 Hz input; the dot moves upwards is 25Hz.

means that the neuron receives p_c out of p Poisson processes of firing rates of 25 Hz (upward motion) or 75 Hz (downward motion) and $p - p_c$ Poisson processes of random firing rates uniformly taking values from 0 to 100 Hz.

The parameters used in simulating the IF model are $V_{thre} = 20mV$, $V_{rest} = 0mV, L = 1/20$, $a = b = 1mV, p = 100, \lambda_1 = 25$ Hz and $\lambda_2 = 75$ Hz. A refractory period of 5msec is added for all numerical results of efferent firing frequency. For each fixed set of parameters of the model, 100 spikes are generated to calculate each mean, standard deviation etc.

Fig. 3 depicts the histogram of firing rates with purely excitatory $r = 0$ (left column) and almost balanced excitatory and inhibitory inputs $r = 0.95$ (right column)

with $c = 0.1$ [21] and $p_c = 15$ (upper panel), 25 (bottom panel). It is easily seen that when $p_c = 25$ and $r = 0.95$, from an observation of single neuron activity, we could perfectly separate upward from downward motions. Nevertheless, when $r = 0$ and $p_c = 25$ we are not able to perfectly separate upward from downward motions.

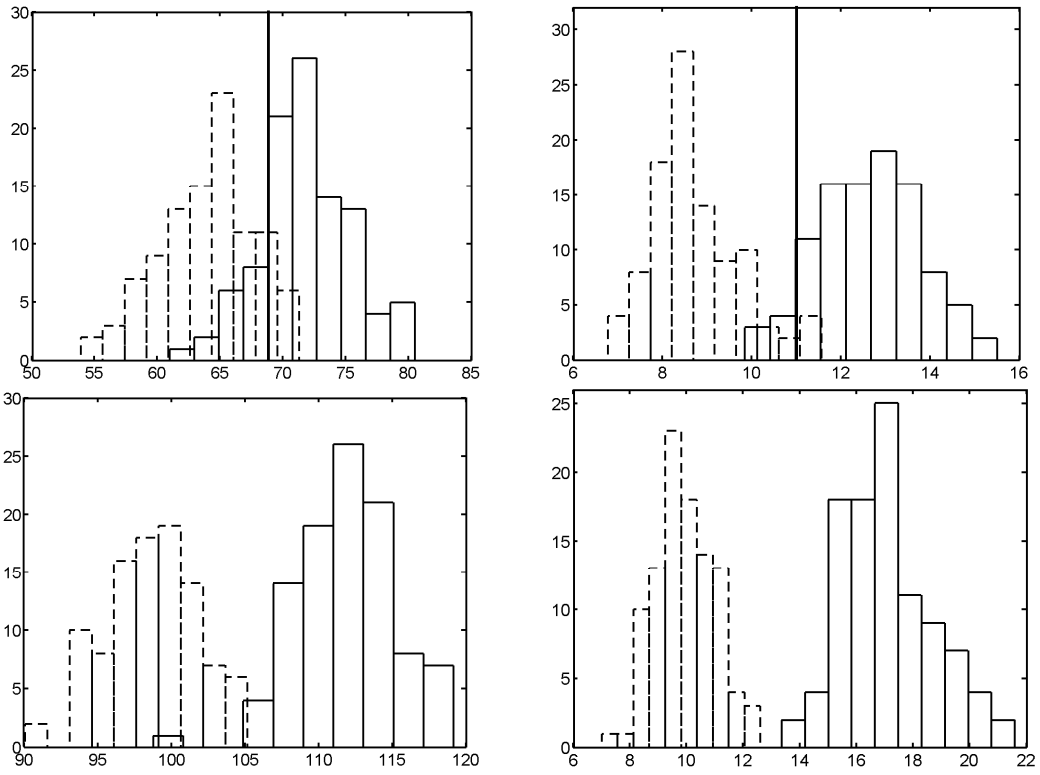

Figure 3: Histogram of firing rates (Hz) with $c = 0.1$ for the IF model. Left, exclusively excitatory inputs $r = 0$. Right, $r = 0.95$. Upper panel: $p_c = 15$. The minimum TPM is calculated according to the thick vertical lines (the optimal discrimination line). Bottom panel: $p_c = 25$.

Let us now consider the minimum total probability of misclassification (TPM) defined by

$$\text{TPM} = \frac{1}{2}P(\text{ downward }|\text{input is upward}) + \frac{1}{2}P(\text{ upward }|\text{input is downward})$$

For example, in Fig. 3, we see that TPM (in percentile) for the left upper panel is

about 13.5% and for the right upper panel is 5.5%. Therefore adding inhibitory inputs to the neuron considerably improves its discrimination capability, reducing TPM from 13.5% to 5.5%.

In Fig. 4 the histogram of coefficient of variation (CV) of efferent spike trains is plotted. Our results also reveal one possible functional role of efferent spike trains with a high CV widely observed in experiments. In the past few years, there are a large body of literatures devoted to the topic: how to generate efferent spike trains with a large CV for the IF model(see [6] for a review). Nevertheless, the functional implications of efferent spike trains with a large CV are still not clear. Here we find that for a fixed coherence level, a lower TPM value corresponds to a larger CV. In other words, for a given p_c, to achieve a better discrimination naturally requires that efferent spike trains are more irregular.

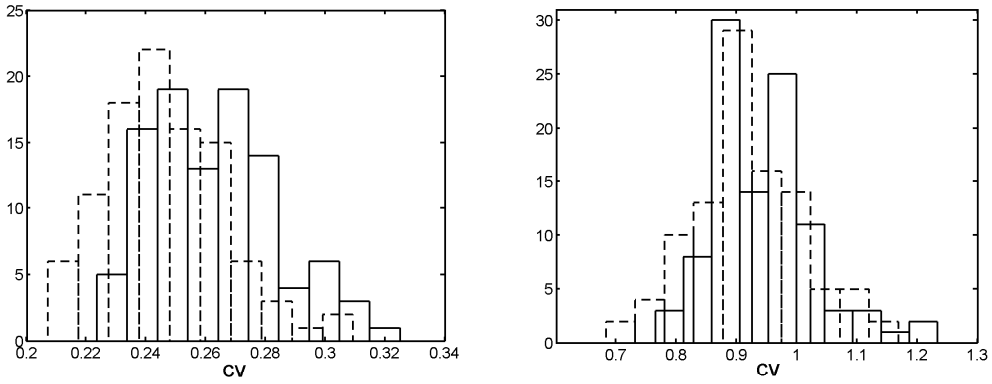

Figure 4: Histogram of CV with $c = 0.1, p_c = 15$ for the IF model. Left, exclusively excitatory inputs $r = 0$. Right, $r = 0.95$.

In Fig. 5 we plot TPM (in percentile) vs. p_c for $r = 0$ and $r = 1$ and TPM vs. r for $p_c = 15$ and $p_c = 25$. TPM vs. p_c simply confirms our conclusion that adding inhibitory inputs improves a neuron's capability of discriminating between different inputs. Remember that the noise strength in the input (σ defined in Eq. (3.1)) is proportional to r. The larger the r is, the larger the input noise. TPM vs. r in Fig. 5 tells us another interesting phenomenon: increasing noise in the model is useful rather

than harmful. The benefit of noise in neuronal system has been extensively explored in the literature of stochastic resonance [8]. However, the mechanism to reach the finely tuning noise level which results in the stochastic resonance seems far-fetched for neuronal systems. Our finding here provides a more direct and convincing evidence which clearly demonstrates the advantage of adding noise to a neuronal system.

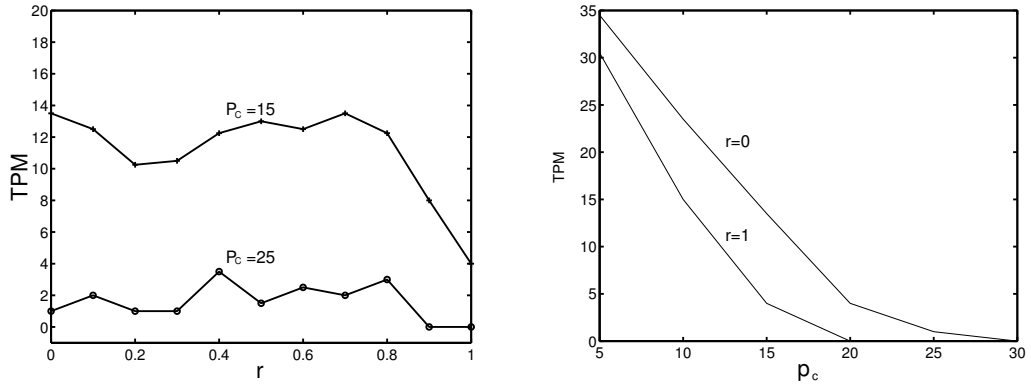

Figure 5: TPM % vs. r (left) and TPM vs. p_c (right) for the IF model. When $p_c = 15$ (left), it is clearly shown that TPM attains its optimal value at $r = 1$, i.e. the larger the noise, the better the discrimination (see the right figure as well).

3.1 Other Input Forms

The results presented in the previous subsections seems quite count-intuitive since we all know that adding inhibitory inputs to the IF model increases its CV of efferent spike trains. Namely increasing inhibitory inputs to the model will make the histogram of firing rates more widely spread out and so make the discrimination task more difficult. In this subsection, we consider the model with other forms of inputs.

The input in the previous subsection is

$$\begin{aligned} di_{syn}(t) &= a(p_c\lambda_j + \sum_{i=1}^{p-p_c}\xi_i)(1-r)dt \\ &\quad + a\sqrt{[\lambda_j p_c(1+c(p_c-1)) + \sum_{i=1}^{p-p_c}\xi_i](1+r)}\cdot dB_t \\ &= \mu dt + \sigma dB_t \end{aligned} \tag{3.1}$$

where $j = 1, 2$. From results in [6] we know that

$$\langle T\rangle = \frac{2}{L}\int_{\frac{V_{rest}L-\mu}{\sigma}}^{\frac{V_{thre}L-\mu}{\sigma}} g(x)dx \tag{3.2}$$

where

$$g(x) = \left[\exp(x^2)\int_{-\infty}^{x}\exp(-u^2)du\right]$$

In terms of the law of large numbers we conclude that

$$\sum_{i=1}^{p-p_c}\xi_i \sim (p-p_c)\langle\xi_1\rangle + \sqrt{p-p_c}\xi\sigma(\xi_1) \tag{3.3}$$

where $\sigma(\xi_1)$ is the standard deviation of ξ_1 and $\xi \sim N(0,1)$.

Hence Eq. (3.2) turns out to be

$$\begin{aligned} \langle T\rangle = \frac{2}{L} & \\ \cdot \int_{\frac{V_{thre}L - a[p_c\lambda_j + (p-p_c)\langle\xi_1\rangle + \sqrt{p-p_c}\xi\sigma(\xi_1)](1-r)}{a\sqrt{[\lambda_j p_c(1+c(p_c-1)) + (p-p_c)\langle\xi_1\rangle + \sqrt{p-p_c}\xi\sigma(\xi_1)](1+r)}}}^{\frac{-[p_c\lambda_j + (p-p_c)\langle\xi_1\rangle + \sqrt{p-p_c}\xi\sigma(\xi_1)](1-r)}{\sqrt{[\lambda_j p_c(1+c(p_c-1)) + (p-p_c)\langle\xi_1\rangle + \sqrt{p-p_c}\xi\sigma(\xi_1)](1+r)}}} & g(x)dx \end{aligned} \tag{3.4}$$

We have checked the accuracy of the approximation developed here. It is found that the approximation in Eq. (3.4) is not very good (compare Fig. 6 upper panel with Fig. 3 upper panel), simply implying that we have to include more higher order terms in the approximation of Eq. (3.3). Nevertheless, Eq. (3.4) gives us a transparent formula to study the issues discussed in the previous subsection and Eq. (3.4) is exact if we model the input rate as a normally distributed random variable[1] rather than a uniformly distributed random variable.

[1]More exactly, it should be a random variable so that Eq. (3.4) makes sense.

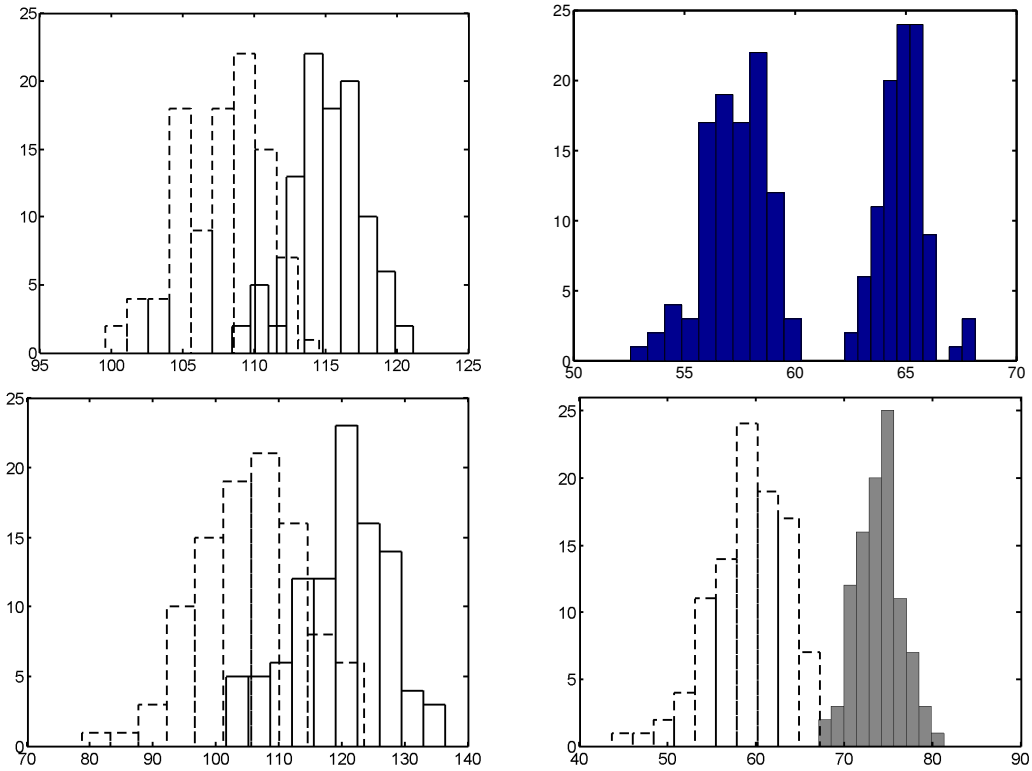

Figure 6: Histogram of firing rates (Hz) with $c = 0.1, p_c = 15, \langle \xi_1 \rangle = 0.05$ and $\sigma(\xi_1) = .1/\sqrt{12}$ (upper panel, compare with Fig.), $p_c = 25$ and $\sigma(\xi_1) = 1/\sqrt{12}$ (bottom panel) for the IF model with inputs defined by Eq. (3.3). Left, exclusively excitatory inputs $r = 0$. Right, $r = 0.95$.

To the first order approximation, Eq. (3.4) reveals the underpinning mechanism of the phenomena observed here. From Eq. (3.4) we have

$$\langle T\rangle \sim \langle T_1\rangle = \frac{2g(0)V_{thre}}{a\sqrt{[\lambda_j p_c(1+c(p_c-1))+(p-p_c)\langle\xi_1\rangle+\sqrt{p-p_c}\xi\sigma(\xi_1)](1+r)}} \tag{3.5}$$

The firing rate in the unit of Hz is then

$$= \frac{\frac{1000}{R_e+\langle T_1\rangle}}{\frac{1000a\sqrt{[\lambda_j p_c(1+c(p_c-1))+(p-p_c)\langle\xi_1\rangle+\sqrt{p-p_c}\xi\sigma(\xi_1)](1+r)}}{R_e a\sqrt{[\lambda_j p_c(1+c(p_c-1))+(p-p_c)\langle\xi_1\rangle+\sqrt{p-p_c}\xi\sigma(\xi_1)](1+r)}+g(0)V_{thre}}} \tag{3.6}$$

where R_e is the refractory period. Let us denote $c_1 = p_c(1+c(p_c-1))$ and $c_2(\xi) = (p-p_c)\langle\xi_1\rangle+\sqrt{p-p_c}\xi\sigma(\xi_1)$ then Eq. (3.6) is

$$\frac{1000a\sqrt{[\lambda_j c_1+c_2(\xi)](1+r)}}{R_e a\sqrt{[\lambda_j c_1+c_2(\xi)](1+r)}+g(0)V_{thre}} \tag{3.7}$$

Under the assumption that ξ is a small perturbation of a deterministic quantity or in the sense of the mean field approximation, we have

$$\begin{aligned}&\frac{1000a\sqrt{[\lambda_2 c_1+c_2(\langle\xi\rangle)](1+r)}}{R_e a\sqrt{[\lambda_2 c_1+c_2(\langle\xi\rangle)](1+r)}+g(0)V_{thre}}-\frac{1000a\sqrt{[\lambda_1 c_1+c_2(\langle\xi\rangle)](1+r)}}{R_e a\sqrt{[\lambda_1 c_1+c_2(\langle\xi\rangle)](1+r)}+g(0)V_{thre}}\\ >&\frac{1000a\sqrt{[\lambda_2 c_1+c_2(\langle\xi\rangle)]}}{R_e a\sqrt{[\lambda_2 c_1+c_2(\langle\xi\rangle)]}+g(0)V_{thre}}-\frac{1000a\sqrt{[\lambda_1 c_1+c_2(\langle\xi\rangle)]}}{R_e a\sqrt{[\lambda_1 c_1+c_2(\langle\xi\rangle)]}+g(0)V_{thre}}\end{aligned} \tag{3.8}$$

where $r>0$ and $\lambda_1<\lambda_2$. Therefore we conclude that larger the inhibition is, the more widely separate the firing rate with different inputs and so the easier to discriminate between different input signals. The conclusions are only true under very restricted conditions as specified above, however we would like to show it here since all proofs are straightforward. To have a rigorous result, we have to find the distribution density of $\langle T\rangle$, which is a hard task. However, in the next section, we develop a theory to get around the difficulty.

Next we are going to test how general or robust are our conclusions in the previous subsections. In Fig. 6 we show histograms of firing rates with $\langle\xi_1\rangle = 0.05$, but with

$\sigma(\xi_1) = .1/\sqrt{12}$ (upper panel) and $\sigma(\xi_1) = 1/\sqrt{12}$ (bottom panel). When $\langle\xi_1\rangle = 0.05$ and $\sigma(\xi_1) = .1/\sqrt{12}$, the mean and variance are the same as in the model considered in the previous subsections. When $\langle\xi_1\rangle = 0.05$ and $\sigma(\xi_1) = 1/\sqrt{12}$, the standard deviation of inputs is enlarged by a factor of 10, in comparison with the setup in the previous subsections. It is easily seen that increasing the variance in input signals will make the histograms of firing rates more widely spread out, as shown in Fig. 6, bottom panel. Nevertheless, when $p_c = 25$ we see that the input signals can be perfectly separated.

3.2 Models With Reversal Potentials

A slightly more general model than the IF model defined above is the IF model with reversal potentials defined by

$$dZ_t = -(Z_t - V_{rest})Ldt + d\bar{I}_{syn}(Z_t, t) \tag{3.9}$$

where

$$\bar{I}_{syn}(Z_t, t) = \bar{a}(V_E - Z_t)\sum_{i=1}^{p} E_i(t) + \bar{b}(V_I - Z_t)\sum_{j=1}^{q} I_j(t)$$

V_E and V_I are the reversal potentials $V_I < V_{rest} < V_E$, $\bar{a}(V_E - V_{rest}), \bar{b}(V_I - V_{rest})$ are the magnitude of single EPSP and IPSP when $Z_t = V_{rest}$. We could rewrite Eq. (3.9) in the following form

$$\begin{aligned} dZ_t &= -(Z_t - V_{rest})(Ldt + \bar{a}\sum_{i=1}^{p} dE_i(t) + \bar{a}\sum_{i=1}^{p} dI_i(t)) \\ &\quad +\bar{a}(V_E - V_{rest})\sum_{i=1}^{p} dE_i(t) + \bar{b}(V_I - V_{rest})\sum_{j=1}^{q} dI_j(t) \\ &= -(Z_t - V_{rest})[Ldt + \bar{a}\sum_{i=1}^{p} dE_i(t) + \bar{b}\sum_{i=1}^{p} dI_i(t)] \\ &\quad +a\sum_{i=1}^{p} dE_i(t) + b\sum_{j=1}^{q} dI_j(t) \end{aligned} \tag{3.10}$$

Therefore the difference between the model with and without reversal potentials is that the latter has a decay rate depending on incoming signals. From the conclusions of

the previous subsections we would expect that the model with reversal potentials will improve its capacity of discriminating incoming signals.

Fig. 7 is in agreement with our expectations. We see that for $p_c = 15$ and $r = 0.6$ a perfect discrimination is achieved. For the model without reversal potentials, we see that for $p_c = 15$ and $r = 1$ we still have TPM > 0 (see previous subsections). The parameters used in the model with reversal potentials are $\bar{a} = 0.01, \bar{b} = 0.1, V_E = 100mV, V_I = -10mV$, with all other parameters as the model without reversal potentials.

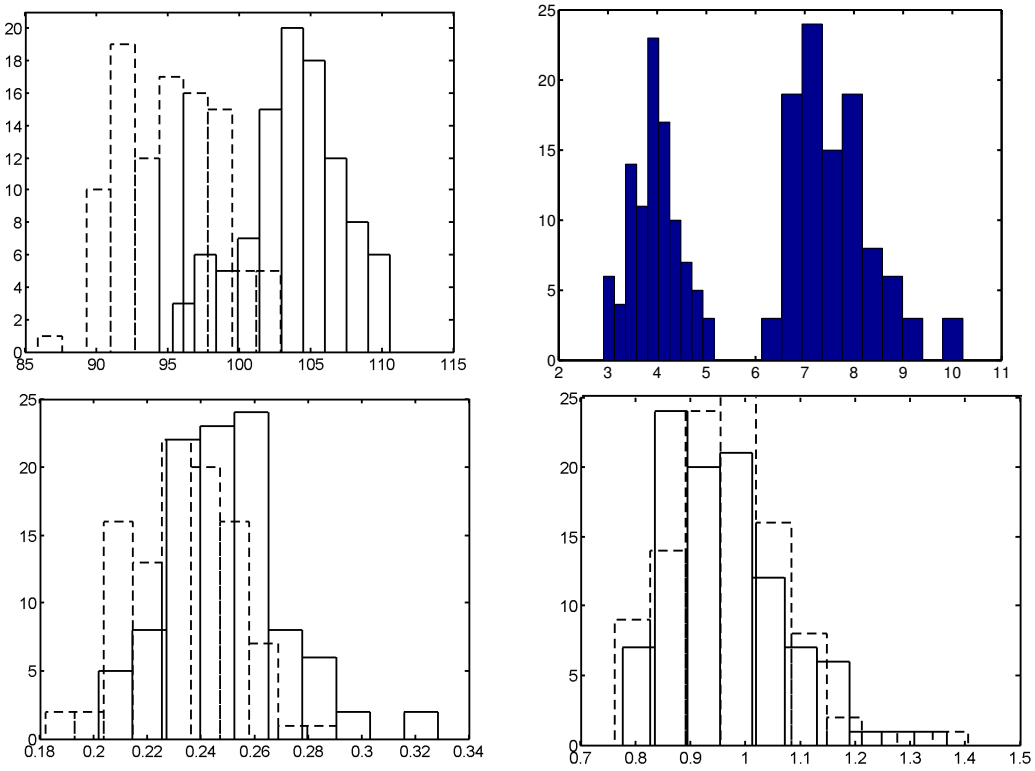

Figure 7: Histogram of firing rates in the unit of Hz (upper panel) and CV (bottom panel) with $c = 0.1, p_c = 15$ for the IF model with reversal potentials. Left, exclusively excitatory inputs $r = 0$. Right, $r = 0.6$.

3.3 IF-FHN Model

The IF model is the simplest neuron model which mimics certain properties of a biological neuron and is linear before resetting. A slightly more complex model is the IF-FHN model, an IF model but with a nonlinear leakage coefficient, as in a biophysical model. In terms of the output signal-to-noise ratio, we know that the IF and IF-FHN model behave in totally opposite ways when they receive correlated inputs (see [6] for a review). We then naturally ask that whether the phenomenon observed in the previous section with partially correlated inputs is true only for the IF model or not. To this end we simulate the IF-FHN model defied by

$$\frac{dv(t)}{dt} = -(1/\beta + \gamma\alpha)v(t) + \gamma(1+\alpha)\frac{v(t)^2}{60} - \frac{\gamma v(t)^3}{3600} + \frac{di_{syn}(t)}{dt} \tag{3.11}$$

when $v(t) < v_{thre} = 50$. The parameters are $v_{rest} = 0, \gamma = 50, \alpha = 0.2, \beta = 2.5$, $a = 2., p = 300$. Note that to ensure the output firing rates in the similar regions for different models, the value of p and a used in the IF-FHN model is higher than that in the IF model, but still in the physiologically plausible regions.

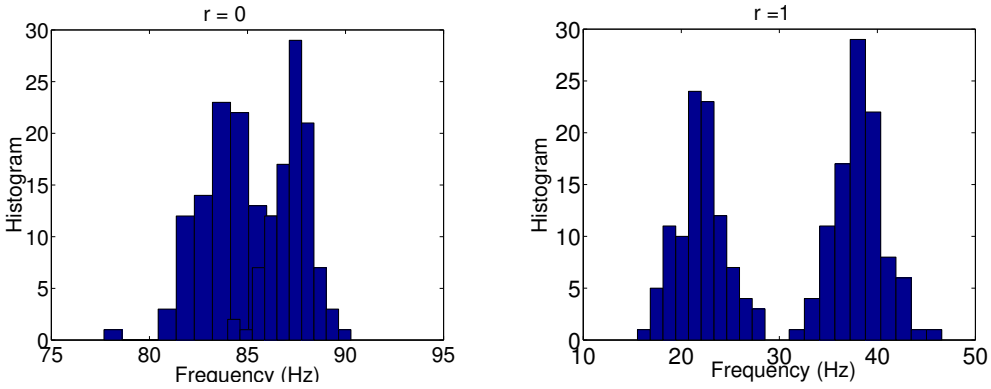

Figure 8: Histogram of efferent frequency (Hz) of the IF-FHN model with $c = 0.1, p_c = 25, p = 300$. Left, exclusively excitatory inputs $r = 0$. Right, $r = 1$.

Fig. 8 shows the simulation results. It is readily seen that all conclusions in the previous section remain true: increasing inhibitory inputs considerably improves the

discrimination capability of the model neuron. Furthermore, the fraction of coherent inputs which ensures a perfect discrimination is less than that of the IF model. For example, in Fig. 8, with $p_c/p = 25/300$ of coherent inputs the histograms of efferent frequency are well separated when $r = 1$.

4 Theoretical Results

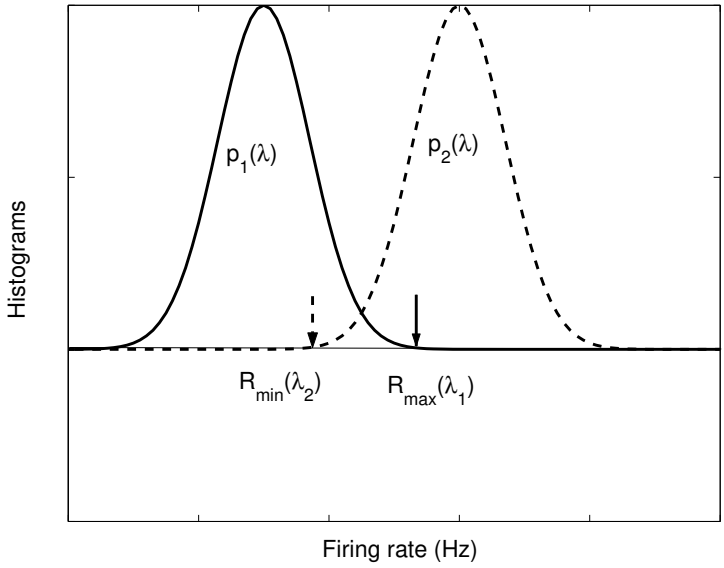

Figure 9: A schematic plot of two output histograms, $R_{\min}(\lambda_2)$ and $R_{\max}(\lambda_1)$.

In this section we concentrate on theoretical results. Let Λ be the set of input frequency of the model, which is $[0, 100]$. It will become obvious that all theoretical results are independent of this choice. For a fixed $(\lambda_1 \in \Lambda, \lambda_2 \in \Lambda)$ with $\lambda_1 < \lambda_2$ we have corresponding two histograms $p_1(\lambda)$ and $p_2(\lambda)$ of output firing rates as shown in Fig. 9. Let

$$R_{\min}(\lambda_2) = \min\{\lambda : \ p_2(\lambda) > 0\}$$

and

$$R_{\max}(\lambda_1) = \max\{\lambda : \ p_1(\lambda) > 0\}$$

and denote

$$\alpha(\lambda_1, \lambda_2, c, r) = \{p_c : R_{\min}(\lambda_2) = R_{\max}(\lambda_1)\} \tag{4.1}$$

If it is clear from the context about the dependence of $\alpha(\lambda_1, \lambda_2, c, r)$ on c, r, we sometimes simply write $\alpha(\lambda_1, \lambda_2, c, r)$ as $\alpha(\lambda_1, \lambda_2)$. Hence for fixed (λ_1, λ_2), $\alpha(\lambda_1, \lambda_2)$ gives us the critical value of p_c: when $p_c > \alpha(\lambda_1, \lambda_2)$ the input patterns are perfectly separable in the sense that the the output firing rate histograms are not mixed with TPM=0; when $p_c < \alpha(\lambda_1, \lambda_2)$ the input patterns might not be separable with TPM> 0. Note that we consider the worst case here and in practical applications, the critical value of p_c at which the input patterns are perfectly separable, as found in the previous section, is in general lower than $\alpha(\lambda_1, \lambda_2, c, r)$. From now on, all figures are generated using the same parameters as in the previous section, if not specified otherwise.

Here is the basic idea of our approach. As pointed out before, it is not easy to directly calculate the distribution of $\langle T \rangle$. Nevertheless, the discrimination task is only involved in the most left point of $p_2(\lambda)$, i.e. $R_{\min}(\lambda_2)$, and the most right point of $p_1(\lambda)$, i.e. $R_{\max}(\lambda_1)$, provided that both p_2 and p_1 are positive only in a finite region. This is exactly the case for the model we considered here since neurons fire within a finite region.

4.1 Behaviour of $\alpha(\lambda_1, \lambda_2, c, r)$

First of all, we want to explore the behaviour of $R_{\min}(\lambda_2) - R_{max}(\lambda_1)$. In Fig. 10, Diff $= R_{\min}(\lambda_2) - R_{max}(\lambda_1)$ with different values of a and $\lambda_1 = 25$Hz,$\lambda_2 = 75$Hz are shown. In all cases we see that it is an increasing function of r and $\alpha(\lambda_1, \lambda_2, c, r)$ is a decreasing function of r.

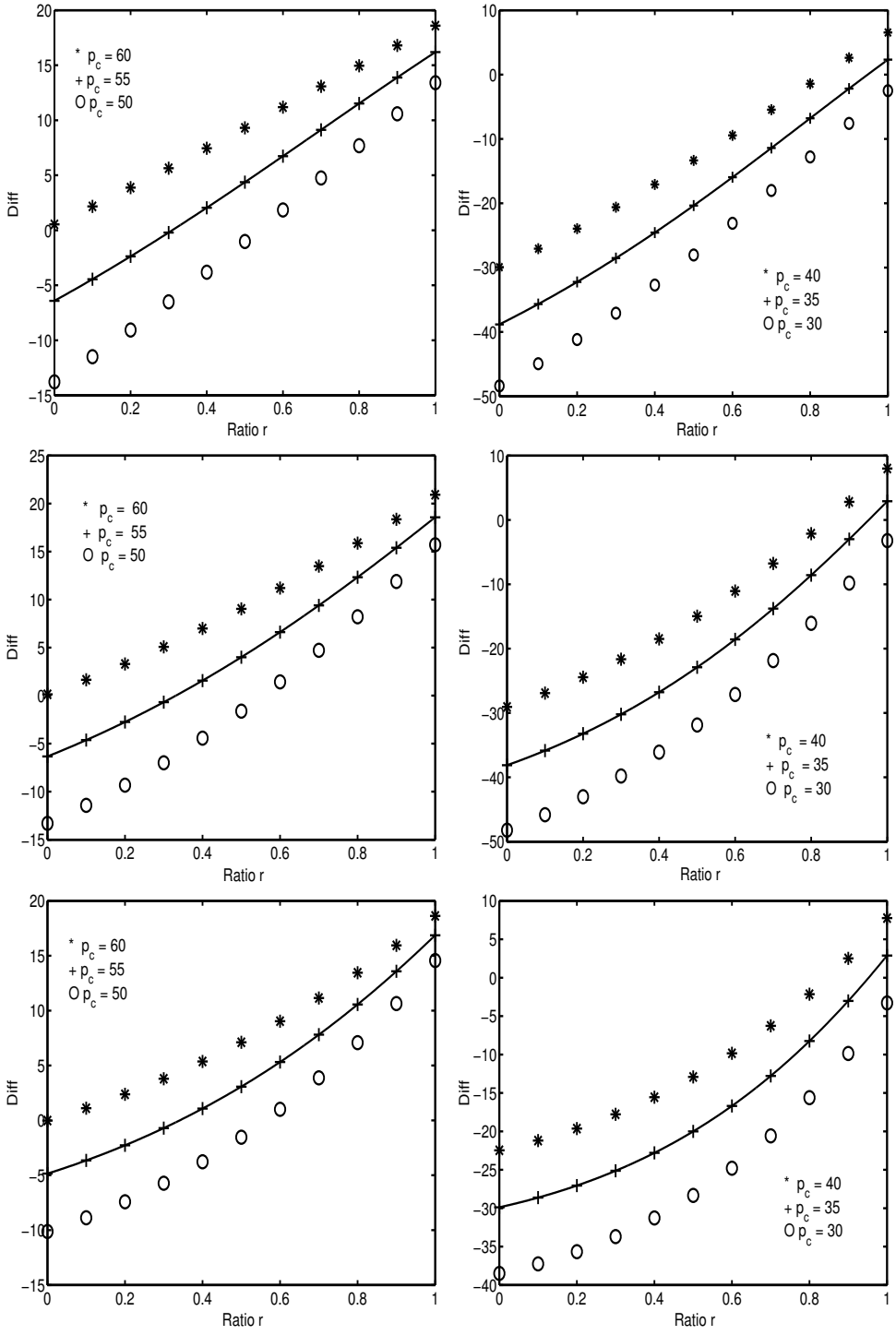

Figure 10: Diff=$R_{\min}(\lambda_2) - R_{max}(\lambda_1)$ for $a = 0.5$ (upper panel), $a = 1$ (middle panel) $a = 2$ (bottom panel) with $\lambda_1 = 25$ Hz, $\lambda_2 = 75$ Hz and $c = 0.1$. It is easy to read out $\alpha(\lambda_1, \lambda_2, c, r)$.

Theorem 1 *Let* $\lambda_{max} = max\{\lambda \in \Lambda\} = 100$ *Hz, we have*

$$\begin{aligned}\alpha(\lambda_1,\lambda_2) &= \left\{p_c : \int_0^{V_{thre}L} g\left(\frac{y - a[p_c\lambda_1 + (p-p_c)\lambda_{\max}](1-r)}{a\sqrt{[\lambda_1 p_c(1+c(p_c-1)) + (p-p_c)\lambda_{\max}](1+r)}}\right)dy\right. \\ &= \frac{\sqrt{[\lambda_1 p_c(1+c(p_c-1)) + (p-p_c)\lambda_{\max}]}}{\sqrt{[\lambda_2 p_c(1+c(p_c-1))]}} \\ &\quad \left.\cdot \int_0^{V_{thre}L} g\left(\frac{y - a(p_c\lambda_2)(1-r)}{a\sqrt{[\lambda_2 p_c(1+c(p_c-1))](1+r)}}\right)dy\right\}\end{aligned} \tag{4.2}$$

Proof As in the previous section we know that

$$\langle T\rangle = \frac{2}{L}\int_{\frac{V_{rest}L-\mu}{\sigma}}^{\frac{V_{thre}L-\mu}{\sigma}} g(x)dx \tag{4.3}$$

where

$$g(x) = \left[\exp(x^2)\int_{-\infty}^{x}\exp(-u^2)du\right]$$

Hence Eq. (4.3) turns out to be

$$\langle T\rangle = \frac{2}{L}\cdot\int^{\frac{V_{thre}L - a[p_c\lambda_j + \sum_{i=1}^{p-p_c}\xi_i](1-r)}{a\sqrt{[\lambda_j p_c(1+c(p_c-1)) + \sum_{i=1}^{p-p_c}\xi_i](1+r)}}} \frac{-[p_c\lambda_j + \sum_{i=1}^{p-p_c}\xi_i](1-r)}{\sqrt{[\lambda_j p_c(1+c(p_c-1)) + \sum_{i=1}^{p-p_c}\xi_i](1+r)}}\ g(x)dx \tag{4.4}$$

Define

$$T(x) = \frac{2}{L}\cdot\int^{\frac{V_{thre}L - a[p_c\lambda_j + x](1-r)}{a\sqrt{[\lambda_j p_c(1+c(p_c-1)) + x](1+r)}}} \frac{-[p_c\lambda_j + x](1-r)}{\sqrt{[\lambda_j p_c(1+c(p_c-1)) + x](1+r)}}\ g(x)dx \tag{4.5}$$

we intend to prove that $T(x)$ is a decreasing function of x. Intuitively it is obvious: the stronger the input is, the shorter the interspike interval. Nevertheless, we have proved in [6] that, in certain circumstances, increasing inhibitory inputs can increase the firing rate. We thus prefer to present a rigorous proof here. From Eq. (4.5) we obtain

$$\begin{aligned}T(x) &= \frac{2}{La\sqrt{[\lambda_j p_c(1+c(p_c-1)) + x](1+r)}} \\ &\quad \cdot\int_0^{V_{thre}L} g\left(\frac{y - a[p_c\lambda_j + x](1-r)}{a\sqrt{[\lambda_j p_c(1+c(p_c-1)) + x](1+r)}}\right)dy\end{aligned} \tag{4.6}$$

Hence the derivative of the second term in Eq. (4.6) is

$$\begin{aligned}
& \frac{2}{L}\cdot\int_0^{V_{thre}L} g'\left(\frac{y-a[p_c\lambda_j+x](1-r)}{a\sqrt{[\lambda_j p_c(1+c(p_c-1))+x](1+r)}}\right) \\
& \qquad \cdot\frac{-2a(1-r)[\lambda_j p_c(1+c(p_c-1))+x](1+r)-(y-a[p_c\lambda_j+x](1-r)(1+r)}{2a(\sqrt{[\lambda_j p_c(1+c(p_c-1))+x](1+r)})^3}dy \\
\leq\ & \underline{g'}\frac{[-2a[\lambda_j p_c(1+c(p_c-1))+x]-(0.5(V_{thre}L)-a[p_c\lambda_j+x])](1-r^2)V_{thre}L}{2a[\sqrt{[\lambda_j p_c(1+c(p_c-1))+x](1+r)}]^3} \\
<\ & 0
\end{aligned}$$

provided that $\underline{g'}>0$ where $\underline{g'}$ is the minima of $g'(x)$ over any compact set. Hence what remains to prove is that $g'(x)>0$ for $x\in R$. When $x\geq 0$, we have

$$g'(x)=2xg(x)+1$$

which implies that $g(x)$ is an increasing function of x. When $x<0$, with integration by part, it can be easily shown that

$$g'(x)=-x\exp(x^2)\int_{-\infty}^{x}\frac{1}{u^2}\exp(-u^2)du>0$$

Hence $g(x)$ is strictly increasing for $x\in R$ and the conclusion is independent of λ_j. Define

$$\begin{aligned}
\tilde{T}(x,p_c,\lambda) &= \frac{2}{La\sqrt{[\lambda p_c(1+c(p_c-1))+x](1+r)}} \\
&\quad\cdot\int_0^{V_{thre}L} g\left(\frac{y-a[p_c\lambda+x](1-r)}{a\sqrt{[\lambda p_c(1+c(p_c-1))+x](1+r)}}\right)dy
\end{aligned} \tag{4.7}$$

we therefore conclude that

$$R_{\min}(\lambda_2)=\frac{1000}{R_e+\tilde{T}(0,p_c,\lambda_2)} \tag{4.8}$$

and

$$R_{\max}(\lambda_1)=\frac{1000}{R_e+\tilde{T}((p-p_c)\lambda_{\max},p_c,\lambda_1)} \tag{4.9}$$

where R_e is the refractory period. Hence the conclusion of the theorem follows.

As we have mentioned before, to find the distribution or the variance of $\langle T\rangle$ is a formidable task. Here, based upon the basic observations that

- The output firing rate is an increasing function of inputs
- Input firing rate is confined within a finite region, which is of course the case in neuroscience

we simplify our task from finding out the variance of $\langle T \rangle$ to solving an algebra equation defined in Theorem 1. Theorem 1 is the starting point of all following results.

Theorem 2 *When $c = 0$ we have*

$$\alpha(\lambda_1, \lambda_2, 0, r) = \frac{p\lambda_{\max}}{\lambda_2 - \lambda_1 + \lambda_{\max}}$$

independent of r. When $c > 0$ we have

$$\alpha(\lambda_1, \lambda_2, c, r_2) < \alpha(\lambda_1, \lambda_2, c, r_1) < \alpha(\lambda_1, \lambda_2, 0, r) \tag{4.10}$$

where $1 \geq r_2 > r_1 > 0$ and furthermore

$$\alpha(\lambda_1, \lambda_2, c, 1) = \frac{\sqrt{[(\lambda_2 - \lambda_1)(1-c) + \lambda_{max}]^2 + 4p\lambda_{\max}c(\lambda_2 - \lambda_1)} - (\lambda_2 - \lambda_1)(1-c) - \lambda_{\max}}{2c(\lambda_2 - \lambda_1)} \tag{4.11}$$

Before proving the conclusions, we first discuss the meaning of Theorem 2. The first conclusion tells us that with $c = 0$, no matter how strong the inhibitory inputs are, the critical value of p_c is independent of r. In other words, without correlated inputs, increasing inhibitory inputs does not enhance the discrimination capacity of the neuron. In Theorem 3 below, we will further prove that without correlated inputs, if the inputs are separable, so are the outputs and vise versa. The second conclusion says that the discrimination capacity of the neuron is improved if the neuron received correlated inputs. With correlated inputs, increasing inhibitory inputs does enhance the discrimination capacity of the neuron. In particular, we see that for a fixed $c > 0$, the optimal discrimination capacity is attained when $r = 1$. Hence Theorem 2 confirms our numerical results on the IF model presented in the previous section.

To prove Theorem 2, at a first glance, we might want to prove that $\alpha(\lambda_1, \lambda_2, r, c)$ is a decreasing function of r. Again a direct, brute force calculation is very hard, if it is not impossible. In the following we employ a more geometrically oriented proof.

Proof Note that when $c = 0$ we have

$$g\left(\frac{y - a[p_c\lambda_1 + (p - p_c)\lambda_{\max}](1 - r)}{a\sqrt{[\lambda_1 p_c + (p - p_c)\lambda_{\max}](1 + r)}}\right) = g\left(\frac{y - a(p_c\lambda_2)(1 - r)}{a\sqrt{\lambda_2 p_c(1 + r)}}\right)$$

independent of r provided that

$$\lambda_1 p_c + (p - p_c)\lambda_{\max} = \lambda_2 p_c$$

which implies the first conclusion.

We postpone the proof of

$$\alpha(\lambda_1, \lambda_2, c, 0) < \alpha(\lambda_1, \lambda_2, 0, r)$$

to Theorem 3 below.

Note that $R_{\min}(\lambda_2) = R_{\max}(\lambda_1)$ for $r = 1$ implies

$$\int_0^{V_{thre}L} \left[g\left(\frac{y}{a\sqrt{[\lambda_1 p_c(1 + c(p_c - 1)) + (p - p_c)\lambda_{\max}2]}}\right) - \frac{\sqrt{[\lambda_1 p_c(1 + c(p_c - 1)) + (p - p_c)\lambda_{\max}]}}{\sqrt{[\lambda_2 p_c(1 + c(p_c - 1))]}} \cdot g\left(\frac{y}{a\sqrt{[\lambda_2 p_c(1 + c(p_c - 1))2]}}\right)\right] dy = 0 \tag{4.12}$$

Since g is a strictly increasing function, we have

$$a\sqrt{[\lambda_1 p_c(1 + c(p_c - 1)) + (p - p_c)\lambda_{\max}2]} = a\sqrt{[\lambda_2 p_c(1 + c(p_c - 1))2]} \tag{4.13}$$

and therefore

$$\alpha(\lambda_1, \lambda_2, c, 1) = \frac{\sqrt{[(\lambda_2 - \lambda_1)(1 - c) + \lambda_{\max}]^2 + 4p\lambda_{\max}c(\lambda_2 - \lambda_1)} - (\lambda_2 - \lambda_2)(1 - c) - \lambda_{\max}}{2c(\lambda_2 - \lambda_1)} \tag{4.14}$$

It is easy to verify that

$$\lim_{c \to 0} \alpha(\lambda_1, \lambda_2, c, 1) = \alpha(\lambda_1, \lambda_2, 0, r)$$

for $r \in [0,1]$.

Finally we want to show that when

$$\alpha(\lambda_1,\lambda_2,c,1)=\frac{\sqrt{[(\lambda_2-\lambda_1)(1-c)+\lambda_{\max}]^2+4p\lambda_{\max}c(\lambda_2-\lambda_1)}-(\lambda_2-\lambda_2)(1-c)-\lambda_{\max}}{2c(\lambda_2-\lambda_1)} \tag{4.15}$$

we have $R_{\min}(\lambda_2) < R_{\max}(\lambda_1)$ for $r=0$. To this end we only need to check that

$$\begin{aligned}
&\int_0^{V_{thre}L}\left[g\left(\frac{y-a[\lambda_1 p_c+(p-p_c)\lambda_{\max}]}{a\sqrt{[\lambda_1 p_c(1+c(p_c-1))+(p-p_c)\lambda_{\max}]}}\right)\right. \\
&\left.-\frac{\sqrt{[\lambda_1 p_c(1+c(p_c-1))+(p-p_c)\lambda_{\max}]}}{\sqrt{[\lambda_2 p_c(1+c(p_c-1))]}}\cdot g\left(\frac{y-a[\lambda_2 p_c]}{a\sqrt{[\lambda_2 p_c(1+c(p_c-1))]}}\right)\right]dy \\
=\ &\int_0^{V_{thre}L}\left[g\left(\frac{y-a[\lambda_1 p_c+(p-p_c)\lambda_{\max}]}{a\sqrt{[\lambda_1 p_c(1+c(p_c-1))+(p-p_c)\lambda_{\max}]}}\right)\right. \\
&\left.-g\left(\frac{y-a[\lambda_2 p_c]}{a\sqrt{[\lambda_2 p_c(1+c(p_c-1))]}}\right)\right]dy>0
\end{aligned} \tag{4.16}$$

This is obvious since $a[\lambda_1 p_c+(p-p_c)\lambda_{\max}] < a[\lambda_2 p_c]$. This, together with the fact that $R_{\min}(\lambda_2) - R_{\max}(\lambda_1)$ is an increasing function of p_c, we conclude that all conclusions in Theorem 2 are true.

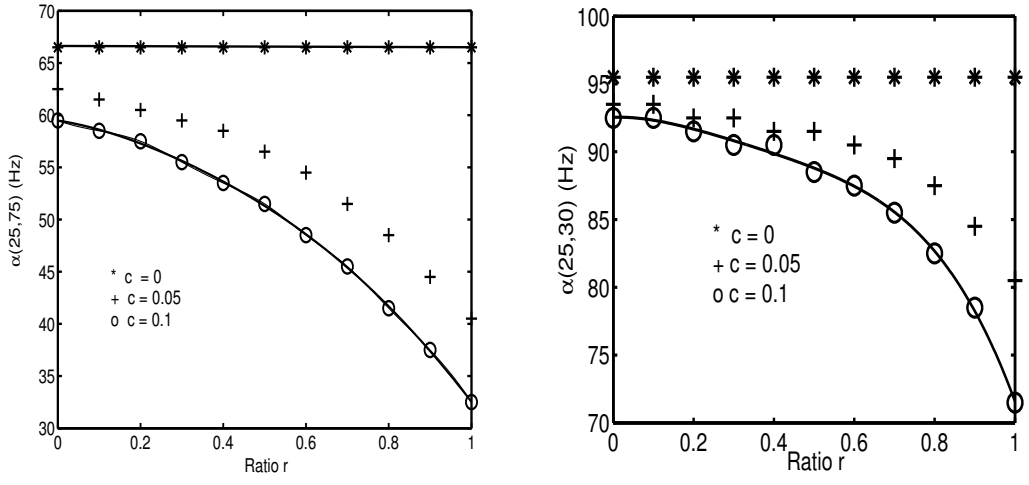

Figure 11: $\alpha(\lambda_1,\lambda_2)$ (Hz) vs. ratio r with $\lambda_1 = 25$ Hz and λ_2=75 Hz and $\lambda_1 = 25$ Hz and λ_2=30 Hz. It is easily seen that when $c=0$, $\alpha(\lambda_1,\lambda_2)$ is flat, otherwise it is a decreasing function of r.

In Fig. 11 some numerical results of $\alpha(\lambda_1, \lambda_2)$ are shown. It is easily seen that when $c = 0$, $\alpha(\lambda_1, \lambda_2)$ is independent of r.

We want to point out another amazing fact from Theorem 2. $\alpha(\lambda_1, \lambda_2, 0, r)$ and $\alpha(\lambda_1, \lambda_2, c, 1)$ with $c > 0$ are both independent of a, V_{thre}, L. When $r = 1, c = 0.1, \lambda_1 =$ 25 Hz, $\lambda_2 = 75$ Hz and $\lambda_{\max} = 100$ Hz and $p = 100$, we have $\alpha(25, 75, 0.1, 1) = 32.5133, \alpha(25, 75, 0, 1) = 66.6667$ (see Fig. 10 and 11). Hence we conclude $32.5133 < \alpha(25, 75, 0.1, r) < 66.6667$ for $r \in (0, 1)$.

Finally we are in the position to answer one of the questions raised in the introduction: a large CV implies a small $\alpha(\lambda_1, \lambda_2, c, r)$. Note that the CV of interspike intervals is the the variance when we calculate the mean interspike intervals. In other words, for each fixed realization of $\xi_i, i = 1, \cdots, p - p_c$, it is the variation of T. When we calculate $\alpha(\lambda_1, \lambda_2, c, r)$, the variance of firing rates histogram is mainly introduced via the masking 'noise'. In other words it is the variation of $\langle T \rangle$. Therefore these are different sources of noise. By increasing the number of interspik intervals, we can reduce the variance of the first kind. Note that in the previous section, we deliberately employ a small number of spikes (100), which might close to the biological reality, to estimate $\langle T \rangle$. The second kind of variance is due to the fluctuation of input signals, or masking noise. In conclusion, increasing inhibitory inputs introduces more variations when we calculate $\langle T \rangle$, but improves neuronal discrimination capacity.

4.2 Input-Output Relationship

In the previous subsections, we only consider the output firing rate histograms. It is certainly interesting to compare the input histograms with output histograms. As before, let Λ be the set of input frequency of the model. For a fixed $(\lambda_1 \in \Lambda, \lambda_2 \in \Lambda)$ with $\lambda_1 < \lambda_2$ we have corresponding two histograms $p_1^i(\lambda)$ and $p_2^i(\lambda)$ of input firing rates, i.e. $p_1^i(\lambda)$ is the histogram of $p_c\lambda_1 + \sum_{i=1}^{p-p_c} \xi_i$ and $p_2^i(\lambda)$ is the histogram of

$p_c\lambda_2 + \sum_{i=1}^{p-p_c} \xi_i$. Define

$$R^i_{\min}(\lambda_2) = \min\{\lambda, p^i_2(\lambda) > 0\}$$

and

$$R^i_{\max}(\lambda_1) = \max\{\lambda, p^i_1(\lambda) > 0\}$$

Then the relationship between $R^i_{\min}(\lambda_2) - R^i_{\max}(\lambda_1)$ and $R_{\min}(\lambda_2) - R_{\max}(\lambda_1)$ characterizes the input-output relationship of neuron signal transformations.

We first want to assess that whether $R_{\min}(\lambda_2) - R_{\max}(\lambda_1) > 0$ even when $R^i_{\min}(\lambda_2) - R^i_{\max}(\lambda_1) < 0$, i.e. the input signal is mixed, but the output signal is separated. In Fig. 12, we plot $R_{\min}(\lambda_2) - R_{\max}(\lambda_1)$ vs $R^i_{\min}(\lambda_2) - R^i_{\max}(\lambda_1) = \lambda_2 p_c - \lambda_1 p_c - \lambda_{max}(p - p_c)$, which is a function of p_c. It is easily seen that after neuronal transformation, mixed signals are better separated when $c > 0$. For example, when $c = 0.1, r = 1$ and $R^i_{\min}(\lambda_2) - R^i_{\max}(\lambda_1) = -5000$ Hz (mixed), but $R_{\min}(\lambda_2) - R_{\max}(\lambda_1) > 0$ (separated). The conclusion is not true for $c = 0$, but the separation is not worse after neuronal transformation.

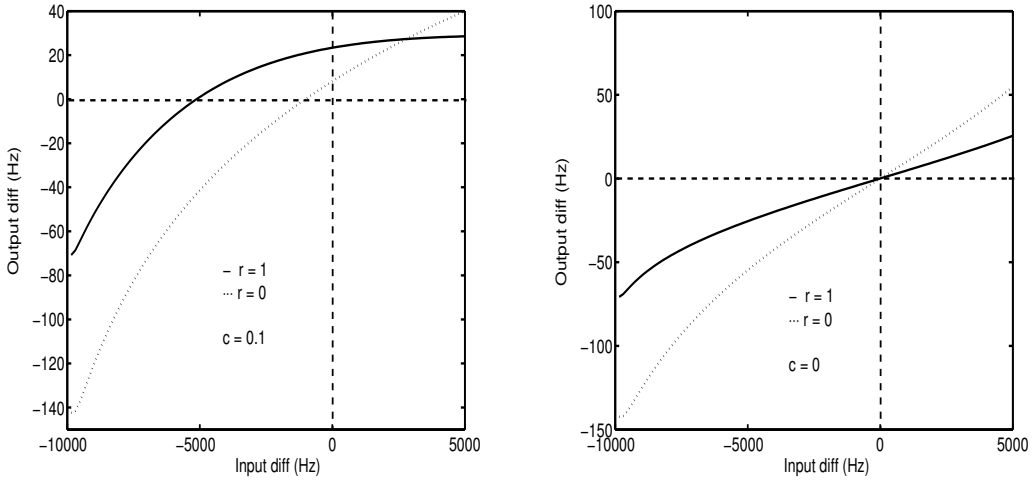

Figure 12: $R_{\min}(\lambda_2) - R_{\max}(\lambda_1)$ vs $R^i_{\min}(\lambda_2) - R^i_{\max}(\lambda_1)$ which is a function of p_c, for $c = 0$ (right) and $c = 0.1$ (left).

Theorem 3 *If $c > 0$ we have*

$$R_{\min}(\lambda_2) - R_{\max}(\lambda_1) > 0 \qquad when \qquad R^i_{\min}(\lambda_2) - R^i_{\max}(\lambda_1) = 0$$

Proof According to the definition of $R^i_{\min}(\lambda_2)$ and $R^i_{\max}(\lambda_1)$ we have $R^i_{\min}(\lambda_2) = p_c\lambda_2$ and $R^i_{\max}(\lambda_1) = p_c\lambda_1 + \lambda_{\max}(p - p_c)$. From the proof of Theorem 1 we conclude that

$$R_{\min}(\lambda_2) - R_{\max}(\lambda_1) = 0 \qquad \text{when} \qquad R^i_{\min}(\lambda_2) - R^i_{\max}(\lambda_1) = 0$$

if $c = 0$. For $c > 0$, it is readily seen that $R_{\min}(\lambda_2) - R_{\max}(\lambda_1) > 0$ if and only if

$$\int_0^{V_{thre}L} \left[g\left(\frac{y - a[p_c\lambda_1 + (p - p_c)\lambda_{\max}](1-r)}{a\sqrt{[\lambda_1 p_c(1 + c(p_c - 1)) + (p - p_c)\lambda_{\max}](1+r)}} \right) - \frac{\sqrt{[\lambda_1 p_c(1 + c(p_c - 1)) + (p - p_c)\lambda_{\max}]}}{\sqrt{[\lambda_2 p_c(1 + c(p_c - 1))]}} \cdot g\left(\frac{y - a[p_c\lambda_2](1-r)}{a\sqrt{[\lambda_2 p_c(1 + c(p_c - 1))](1+r)}} \right) \right] dy \tag{4.17}$$

is greater than zero. Since $p_c\lambda_2 = p_c\lambda_1 + \lambda_{\max}(p - p_c)$ we can rewrite Eq. (4.17) as follows

$$\int_0^{V_{thre}L} \left[g\left(\frac{y - a[p_c\lambda_2](1-r)}{a\sqrt{[\lambda_1 p_c c(p_c - 1)) + p_c\lambda_2](1+r)}} \right) - \frac{\sqrt{[\lambda_1 p_c c(p_c - 1)) + \lambda_2 p_c]}}{\sqrt{[\lambda_2 p_c(1 + c(p_c - 1))]}} \cdot g\left(\frac{y - a[p_c\lambda_2](1-r)}{a\sqrt{[\lambda_2 p_c(1 + c(p_c - 1))](1+r)}} \right) \right] dy \tag{4.18}$$

Again from the proof of Theorem 1 we know that g is an increasing function, by noting $\sqrt{[\lambda_1 p_c c(p_c - 1)) + p_c\lambda_2]} < \sqrt{[\lambda_2 p_c(1 + c(p_c - 1))]}$ we conclude that Eq. (4.18)> 0.

Furthermore, the output difference of firing rates is an increasing function of p_c, this, together with the conclusions above, also implies the remaining results of Theorem 2.

Theorem 3 reveals one of the interesting properties of neuronal transformation. Under the assumption that input signals are correlated, the output signals will be separated even the input signals are mixed. As aforementioned, we believe that the fundamental requirement for a nervous system is to tell one signal from the other. Theorem 3 tells us that after the transformation of the IF neuron, the input signals could be more easily separable.

5 Discussion

We have considered the problem of discriminating between input signals in terms of an observation of efferent spike trains of single neuron. We have demonstrated, both theoretically and numerically, that two key mechanisms to enhance the discrimination capability of the model neuron is to increase inhibitory inputs and correlated inputs. In [10], the authors have theoretically considered discrimination tasks as well. Nevertheless, our approach is very different from theirs. We have concentrated on neuronal mechanisms, but their results are more or less a direct application of results in statistics.

There are many issues to be further explored in the future.

- We have only considered to accomplish the discriminating task and have not included time constrains. Definitely it is of vital importance for a neuronal system to tell one signal from the other within a time window as short as possible.
- We have tested our model with static inputs. It is an interesting question to generalize our results here to time-varying inputs as reported in [15]. Such a study might be helpful to clarify the ongoing debate on the advantages of 'dynamical stimuli' over the 'static stimuli'.
- The input signal used here is very naive. To transform the image of moving dots to input signals specified in the present paper requires a neural network to preprocess the image. Hence to devise a network model (spiking neural networks or Reichardt detector [3]) to reproduce our results is one of our ongoing research topics. We expect that such a study could provide us with a template to compare models with psychophysical experiments.
- A neuronal system without learning is a 'dead' system. In actual situations, we all know that learning is prevailing in neuronal systems. Hence a reasonable learning rule should improve the neuronal capability of discrimination of different input signals. There are several learning rules reported in the literature. To assess the impact of them on discrimination tasks is an intriguing issue.

Discriminating between different input signals is probably more fundamental constrains on the neural system than others such as maximizing input-output information or redundancy reductions, a view recently echoed in [1]. To understand it will reveal principles employed by neuronal systems which remain mysterious to us. The issue discussed here is currently a hot topic in neuroscience (for example see [13]). Our approach provides us with a solid theoretical foundation for further study and we expect that our approach also opens up many interesting questions to be further investigated in the future.

Acknowledgement. Partially supported by a grant from EPSRC(GR/R54569), a grant of the Royal Society and an exchange grant between UK and China of the Royal Society. F. Liu acknowledges the support from NNSF of China 30070208.

References

[1] Barlow H. (2001) Redundancy reduction revisited. *Network* **12** 241-254.

[2] Britten K.H., Shadlen M.N., Newsome, W.T., Celebrini S., and Movshon J.A. (1992) The analysis of visual motion: a comparison of neuronal and psychophysical performance. *J. Neurosci.* **12** 4745-4765.

[3] Borst A. (2000) Models of motion detection. *Nature Neuroscience* **3** 1168-1168.

[4] Brown D., Feng J., and Feerick, S. (1999) Variability of firing of Hodgkin-Huxley and FitzHugh-Nagumo neurons with stochastic synaptic input. *Phys. Rev. Letts.* **82**, 4731-4734.

[5] Feng, J.(1997) Behaviours of spike output jitter in the integrate-and-fire model. *Phys. Rev. Lett.* **79** 4505-4508.

[6] Feng J. (2001) Is the integrate-and-fire model good enough? –a review. *Neural Networks* **14** 955-975.

[7] Feng J. (with G. Leng et al.) (2001) Responses of magnocellular neurons to osmotic stimulation involves co-activation of excitatory and inhibitory input: an experimental and theoretical analysis. *J. Neurosci.* **21** 6967-6977.

[8] Gammaitoni L., Hänggi P., Jung P. and Marchesoni F. (1998) Stochastic resonance. *Reviews of Modern Physics* **70** 224-287.

[9] Grossberg, S, Maass W., and Markram H. (2001) Neural Networks (Special Issue), vol. **14**.

[10] Gold J.I., and, Shadlen M.N. (2001) Neural computations that underlie decisions about sensory stimuli. *Trends In Cognitive Sciences* **5** 10-16.

[11] Hopfield J.J., and Brody C.D. (2000) What is a moment? 'Cortical' sensory integration over a brief interval. *Proc. Natl. Acad. Sci. USA* **97** 13919-13924.

[12] Hopfield J.J., and Brody C.D. (2001) What is a moment? Transient synchrony as a collective mechanism for spatiotemporal integration. *Proc. Natl. Acad. Sci. USA* **98** 1282-1287.

[13] Kast B. (2001) Decisions, decisions ... *Nature* **411** 126-128.

[14] Parker A.J., and Newsome W.T. (1998) Sense and the single neuron: probing the physiology of perception. *Annu. Rev. Neurosci.* **21** 227-277.

[15] Romo R., and Salinas E.(2001) Touch and go: decision mechanisms in somatosensation. *Annu Rev. Neurosci.* **24** 107-137.

[16] Shadlen M.N, and Newsome W.T. (1996) Motion perception: seeing and deciding. *PNAS* **93** 628-633.

[17] Salinas E., and Sejnowski T. (2000) Impact of correlated synaptic input on ouput firing rate and variability in simploe neuron mdoels. *Journal of Neuroscience*, **20**, 6196-6209.

[18] Salinas E., and Sejnowski T. (2001) Correlated neuronal activity and the flow of neural information. *Nature Reviews Neuroscience* **2**, 539-550.

[19] Tuckwell H. C. (1988) *Introduction to Theoretical Neurobiology* Vol 2, Cambridge University Press.

[20] van Vereeswijk C., Abbott L.F., and Ermentrout G.B. (1994) When inhibition not excitation synchronizes neural firing. *Jour. Computat. Neurosci.* **1** 313-321.

[21] Zohary E., Shadlen M.N., and Newsome W.T. (1994) Correlated neuronal discharge rate and its implications for psychophysical performance. *Nature* **370** 140-143.